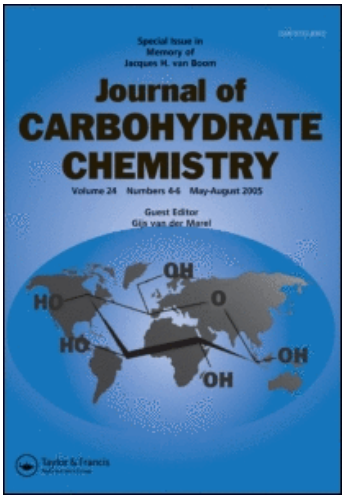

Journal of Carbohydrate Chemistry
Publication details, including instructions for authors and subscription information:
http://www.informaworld.com/smpp/title~content=t713617200

Studies on the Solution Conformation and Dynamics of the Trisaccharide Repeating Unit of the Kps from *Sinorhizobium Fredii* Svq293

Miguel A. Rodríguez-Carvajal; Leandro Gonzalez; Manuel Bernabe; Juan F. Espinosa; José L. Espartero; Pilar Tejero-Mateo; Antonio Gil-Serrano; Jesús Jiménez-Barbero

To cite this Article Rodríguez-Carvajal, Miguel A. , Gonzalez, Leandro , Bernabe, Manuel , Espinosa, Juan F. , Espartero, José L. , Tejero-Mateo, Pilar , Gil-Serrano, Antonio and Jiménez-Barbero, Jesús(1999) 'Studies on the Solution Conformation and Dynamics of the Trisaccharide Repeating Unit of the Kps from *Sinorhizobium Fredii* Svq293', Journal of Carbohydrate Chemistry, 18: 8, 891 — 903
To link to this Article: DOI: 10.1080/07328309908544042
URL: http://dx.doi.org/10.1080/07328309908544042

J. CARBOHYDRATE CHEMISTRY, 18(8), 891–903 (1999)

STUDIES ON THE SOLUTION CONFORMATION AND DYNAMICS OF THE TRISACCHARIDE REPEATING UNIT OF THE KPS FROM *SINORHIZOBIUM FREDII* SVQ293

Miguel A. Rodríguez-Carvajal,[2] Leandro Gonzalez,[1] Manuel Bernabe,[1] Juan F. Espinosa,[1] José L. Espartero,[2] Pilar Tejero-Mateo,[2] Antonio Gil-Serrano,[2] Jesús Jiménez-Barbero[1]*

[1] Instituto Química Orgánica, CSIC, Juan de la Cierva 3, 28006 Madrid
[2] Departamento Química Orgánica, Facultad Química, Univ. Sevilla, 41071-Spain

Received December 3, 1998 - Final Form June 17, 1999

ABSTRACT

The conformational behaviour of the major trisaccharide repeating unit (α-D-Gal*p*-(1→2)-β-D-Rib*f*-(1→9)-α-5-*O*-Me-Kdn*p*-) of the polysaccharide from *Sinorhizobium fredii* SVQ293, a mutant derivative has been analysed by NMR spectroscopy and extensive molecular dynamics simulations. The results obtained indicate that the five-membered ring adopts an almost unique conformation as do the pyranose rings. The Rib*f*-(1→9)-α-5-*O*-Me-Kdn*p* linkage may adopt a variety of conformations while the α-D-Gal*p*-(1→2)-β-D-Rib*f*- also populates an extended surface of the Φ/Ψ map. Two 10 ns MD simulations using the GB/SA continuum solvent model for water and the MM3* force field provides a population distribution of conformers which satisfactorily agrees with the experimental NMR data for both the glycosidic linkages and the hydroxymethyl groups.

INTRODUCTION

The cell wall of gram-negative bacteria consists of the cytoplasmic membrane, or inner membrane, and the outer membrane with a periplasmic space between the two bacterial membranes.[1] The outer membrane is attached via lipoproteins to the peptidoglycan layer, and consists of an asymmetric lipid bilayer with the outer leaflet being formed by the lipid tails of lipopolysaccharide molecules and the inner leaflet being composed of phospholipids and lipoproteins. LPS molecules comprise three major moieties: the lipid A membrane anchor, a core oligosaccharide which is linked to the lipid A via 3-deoxy-D-*manno*-2-octulosonic acid (Kdo), and an antigenic polysaccharide (O-antigen). In addition to lipopolysaccharides, the outer bacterial leaflet contains an acidic polysaccharide called the capsular polysaccharide (or K-antigen, since this polysaccharide carries bacterial cell-surface antigens). K-antigens form an acidic bacterial sheath and are tightly associated with the bacterial cell surface. Rhizobial K-antigen polysaccharides are structurally different from LPS in that, for instance, they contain a higher proportion of Kdo (or compounds closely related to Kdo). To date, no clear functions of rhizobial Kps in the nodulation process have been assigned. However, it has been recently shown that *Sinorhizobium fredii* K-antigens could influence the host specificity for bacterial nodulation.[2]

In a recent publication,[3] we have reported the primary structure of a cell-associated polysaccharide from *Sinorhizobium fredii* SVQ293, a mutant derivative of *Sinorhizobium fredii* HH103 that requires thiamine to grow in minimal media. When bacterial polysaccharides were isolated following the standard protocol for LPS extraction, a new type of capsular polysaccharide (Kps polysaccharide) was identified. This Kps polysaccharide consists of the following trisaccharide repeating unit: →2)-α-D-Gal*p*-(1→2)-β-D-Rib*f*-(1→9)-α-5-*O*-Me-Kdn*p*-(2→. Twenty-five percent of the Kdn residues are not methylated. This Kdn-containing polysaccharide was not detectable in the wild type strain.

We now report on the study of the solution conformation and dynamics of the trisaccharide repeating unit of the mutant polysaccharide, α-D-Gal*p*-(1→2)-β-D-Rib*f*-(1→9)-α-5-*O*-Me-Kdn*p*, using NMR techniques and molecular dynamics simulations.[4] Both the conformation of the pyranose and furanose rings and the orientation around the glycosidic and hydroxymethyl linkages have been analysed.

MOLECULAR MECHANICS AND DYNAMICS CALCULATIONS

Molecular mechanics and dynamics calculations were performed using both the TRIPOS force field[5] within the SYBYL package and the MM3* force field[6] as implemented in MACROMODEL 4.5.[7] Φ_{GR} is defined as Gal-H1 Gal-C1 Gal-O1 Rib-C2 and Ψ_{GR} as Gal-C1 Gal-O1 Rib-C2 Rib-H2. Φ_{RK} is defined as Rib-H1 Rib-C1 Rib-O1 Kdn-C9 and Ψ_{RK} as Rib-C1 Rib-O1 C9 Kdn-C9 Kdn-C8. Only the *gt* orientation[8] of the lateral chain was used for the α-Gal moiety, the three *tg*, *gg* and *gt* orientations were considered for the β-Rib entity. For the 1→9 linkage, the three *tg*, *gg* and *gt* rotamers[8] of the KDN lateral chain were taken into account. Calculations for a dielectric constant ε=80 (SYBYL) and for the continuum GB/SA solvent model (MM3*) were performed.[9] First, potential energy maps were calculated for the constituent disaccharide entities: relaxed (Φ,Ψ) potential energy maps were calculated as described.[10] One initial geometry of the secondary hydroxyl groups of the pyranose moieties was considered, r (counterclockwise). The previous step involved the generation of the corresponding rigid residue maps by using a grid step of 18°. Then, every Φ,Ψ point of this map was optimised using 200 steepest descent steps, followed by 1000 conjugate gradient iterations. From these relaxed maps, the probability distributions calculated for each ϕ, ψ according to a Boltzmann function at 303 K.

Therefore, nine starting structures of trisaccharide 1 were built by combining the three stable conformers[8] of the ribose and Kdn lateral chains and subjected to extensive energy minimization with conjugate gradients. Then, they were used as starting geometries for molecular dynamics (MD) simulations at 300 K. The GB/SA (Generalized Born solvent-accessible surface area) solvent model for water was used for the MM3* simulations, and a bulk dielectric constant of 80 was used for SYBYL. In all cases, the simulations were carried out with a time step of 1 fs. The equilibration period was 100 ps. Structures were saved every 0.5 ps. The total simulation time was 1 ns for every run. Two long 10 ns simulations were also carried out with MM3* for the gg (Ribf)/gt (Kdn) and gg (Ribf)/gg (Kdn) conformers. Average distances between proton pairs were calculated from the MD simulations.

NMR SPECTROSCOPY

NMR experiments were recorded on a Varian Unity 500 spectrometer, using an approximately 12 mM solution of the trisaccharide at different temperatures (betwen

299 and 320 K. The spectra were recorded in D_2O. Chemical shifts are reported in ppm, using external TMS (0 ppm) as reference. The double quantum filtered COSY spectrum was performed using 256 increments of 1K real points to digitize a spectral width of 2000 Hz. Sixteen scans were used with a relaxation delay of 1 s. The 2D TOCSY experiment was performed using a data matrix of 256 increments of 1K real points to digitize a spectral width of 2000 Hz. Four scans were used per increment with a relaxation delay of 2 s. MLEV 17 was used for the 100 ms isotropic mixing time. The one-bond proton-carbon correlation experiment was collected using the gradient enhanced HSQC sequence[11] A data matrix of 256 increments of 1K real points was used to digitize a spectral width of 2000 Hz in F_2 and 10000 Hz in F_1. Four scans were used per increment with a relaxation delay of 1 s and a delay corresponding to a J value of 145 Hz. ^{13}C decoupling was achieved by the WALTZ scheme. The 2D-HMQC-TOCSY experiment was conducted with an 80 ms mixing time (MLEV 17) The same conditions as for the HSQC experiment were employed. HMBC experiments were performed using the gradient enhanced sequence[12] with 256 increments of 2K real points to digitize a spectal width of 2000 * 15000 Hz. Eight scans were acquired per increment with a delay of 65 ms for evolution of long range couplings.

2D NOESY,[13] 2D-ROESY,[14] and 2D-T-ROESY[15] experiments were performed using four different mixing times, namely 150, 300, 450, and 600 ms, with 256 increments of 2K real points. Good linearity was observed up to 200 ms (NOESY) and 300 ms (ROESY). Estimated errors in the NOE intensities are smaller than 20%. 1D-NOESY experiments using the double pulse field gradient spin echo technique[16] were also acquired with the same mixing times.

RESULTS AND DISCUSSION

^1H NMR Data.- Since NMR parameters are time-averaged, the information that is possible to deduce from these experiments corresponds to the time-averaged conformation in solution.

^1H NMR and ^{13}C NMR spectra of **1** were completely assigned by a combination of homonuclear COSY, TOCSY, and heteronuclear HMQC, HMBC, and HMQC-TOCSY techniques. These last two techniques were crucial to solve the final ambiguities. The corresponding ^1H and ^{13}C NMR chemical shifts are listed in Table 1. The pyranose rings of the galactose and Kdnp rings can be described as essentially

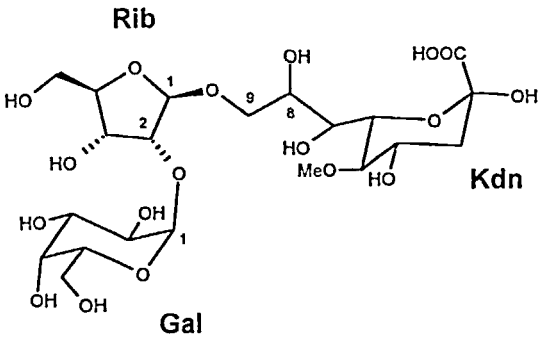

Table 1. ^{1}H and ^{13}C NMR chemical shifts (δ, ppm) of trisaccharide **1**

H-	Ribf	Gal	Kdn	C-	Ribf	Galp	Kdn
H-1	5.13	5.12		C-1	105.8	97.7	177.2
H-2	4.16	3.81		C-2	78.9	68.6	96.9
H-3	4.31	3.91	1.73,2.11	C-3	70.7	69.3	39.8
H-4	4.05	3.95	3.98	C-4	83.4	69.6	69.6
H-5	3.78,3.61	4.07	3.30	C-5	62.8	71.7	80.9
H-6		3.70	3.85	C-6		61.7	70.9
H-7			3.71	C-7			68.6
H-8			3.82	C-8			69.7
H-9			3.97,3.64	C-9			70.3

monoconformational: $^{4}C_1$ and $^{1}C_4$, respectively, as deduced from the vicinal proton proton couplings[17] (Table 2). The couplings for the ribofuranose ring were $J_{1,2}$ 1.0 Hz, $J_{2,3}$ 4.8 Hz, and $J_{3,4}$ 6.9 Hz, indicating a major conformation of this ring, between the E_2 and $^{3}T_2$ forms, similar to the C3'-endo form, usually found in RNA structures. In fact, the expected couplings for the $^{3}T_2$ conformation were $J_{1,2}$ 1.2 Hz, $J_{2,3}$ 4.9 Hz, and $J_{3,4}$ 8.0 Hz (see below under conformational analysis), in excellent agreement with the experimental values. NOESY and ROESY experiments were in agreement with these J data.[17] The couplings for the lateral chains are gathered in Table 3. The observed data indicate equilibria in all cases.[8] In addition, the NOESY/ROESY experiments performed with different mixing times were used to estimate proton/proton interresidue distances.[18] The good linearity observed in the build up curves for NOESY/ROESY spectra warranted the safe application of the isolated spin pair approximation, within

Table 2. Vicinal proton/proton coupling constants for trisaccharide **1** (Hz)

Vicinal Coupling	Rib*f*	Gal*p*	Kdn*p*
H-1/H-2	1.0	3.9	-
H-2/H-3	4.8	10.3	
H-3/H-4	6.9	3.4	12.4, 5.0
H-4/H-5	2.8, 6.0	1.0	9.5
H-5/H-6		4.8, 7.0	
H-6/H-7			2.5
H-7/H-8			8.9
H-8/H-9			2.3, 5.6

Table 3. Experimental (NOE) *vs* MD-simulated interresidue H/H distances.

H/H PAIR	MD	EXP	H/H PAIR	MD	EXP
Gal*p* 1/Rib*f*2	2.80	2.5-2.9	Gal*p* 1/Rib*f*1	2.92	overlap
Gal*p* 5/Rib*f*2	2.89	2.5-2.9	Rib*f*1/Rib*f*4	3.39	3.0-3.4
Rib*f*1/Rib*f*2	3.05	2.7-3.1	Rib*f*2/Rib*f*3	2.4	2.2-2.4
Kdn*p*9$_R$/Rib*f*1	2.54	2.5-2.9	Kdn*p* 9$_S$/Rib*f*1	3.05	2.8-3.2
Rib*f*3 /Rib*f*5$_R$	3.10	2.5-2.9	Rib*f*3 /Rib*f*5$_S$	3.00	2.8-3.2

certain bounds. For **1**, all NOESY cross peaks were positive (Fig. 1) at 500 MHz and 299 K. The distance results are given in Table 3.

Although only approximated, the Gal H-1/H-2 intraresidue signals were used as reference assuming that their separation is 2.5 Å. Thus, the NOEs were first assigned as strong (s), medium (m), and weak (w) and then quantitated. The MD-calculated distances (see below) are shown in the same Table. It can be observed that a good match is observed between the experimental distances and those estimated through molecular mechanics and dynamics simulations.

Conformational Analysis. Molecular Dynamics Studies. As a first step to determine the overall three dimensional structure of the oligosaccharide, molecular mechanics and dynamics calculations were performed. Information on the amount of conformational space accessible was obtained through molecular dynamics simulations[19] of **1**. Simulations with the SYBYL and MM3* programmes were performed, since they have provided satisfactory results in the study of the

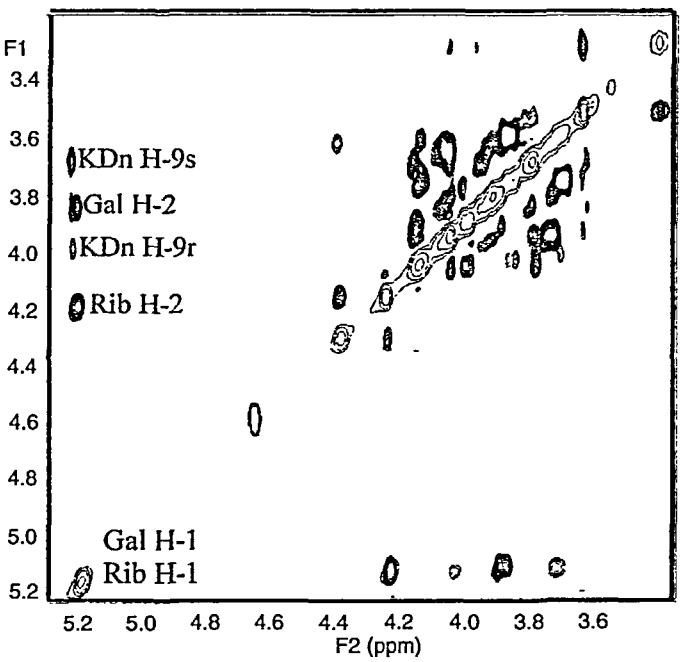

Figure 1. Partial section of a 500 MHz NOESY of **1** at 299 K (mixing time, 300 ms).

conformation of a variety of oligosaccharide molecules.[20] The 2-*O*-substituted five-membered ring converged to one unique structure, close to the ^3E form, in agreement with the experimental vicinal proton-proton couplings discussed above (calculated, $J_{1,2}$ 1.2 Hz, $J_{2,3}$ 4.9 Hz, and $J_{3,4}$ 8.0 Hz). In this conformation, a pseudoequatorial orientation of the C5 hydroxymethyl group is achieved. No important contacts are observable between the Gal and Kdn residues, which could facilitate the existence of this unique conformation. In fact, molecular mechanics calculations carried out for the constituent α-D-Gal*p*-(1→2)-β-D-Rib*f*β-OMe disaccharide also provided the same conformation, indicating that the presence of this conformation is probably due to the existence of a 1,2-di-*O*-substituted Rib*f*β residue. Then, relaxed potential energy maps (Φ/Ψ) were calculated for every glycosidic linkage. The glycosidic linkages present well defined low energy regions, which cover less than 20% of the complete potential energy surface. All the energy regions show Φ values (Table 4) which are centered around

Table 4. Glycosidic and hydroxymethyl torsion angles and their range of variation as deduced from the MD simulations carried out for trisaccharide 1

Torsion	Galp-Rib*f*	Ribf-Kdn*p*
Φ	-45 (-90 → +60)	55 (0 → +90)
Ψ	-60 (-100 → +80)	176 (-60 → +90)

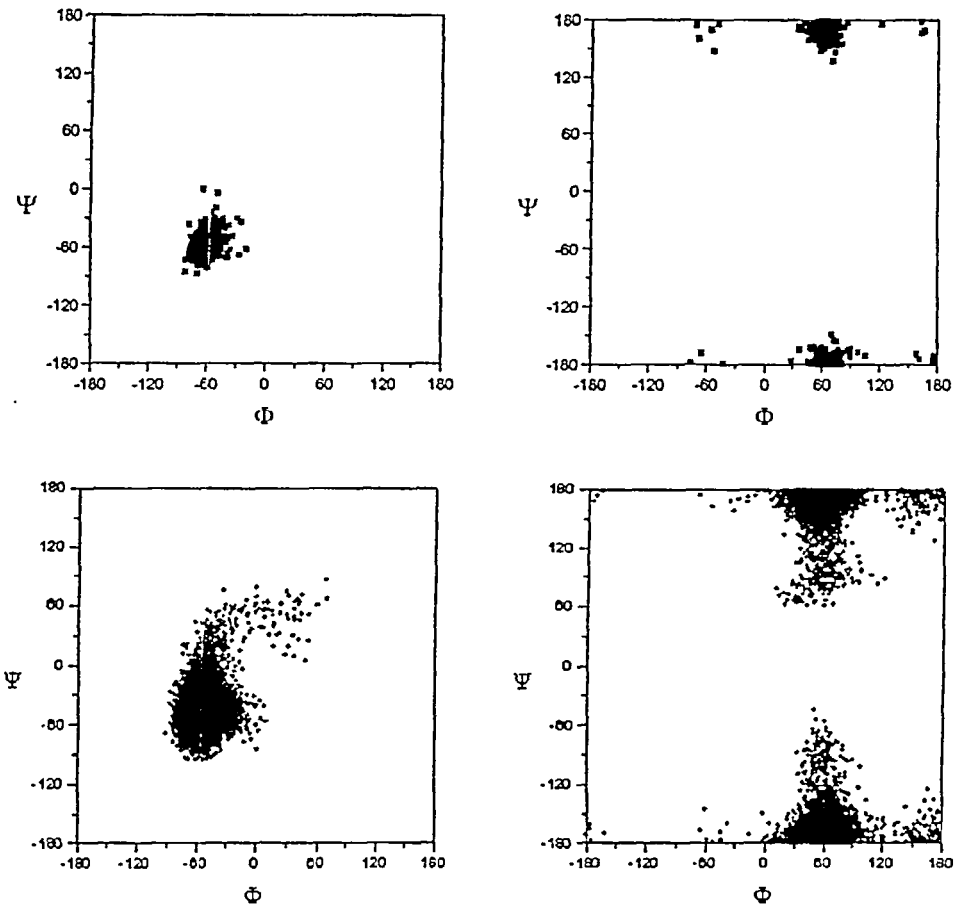

Figure 2. History plots of Φ/Ψ glycosidic torsion angles for both linkages during a 1 ns MD simulation with the TRIPOS force field (top) and one 10 ns simulation with the MM3* force field and the GB/SA model (bottom). An extended surface around the corresponding global minima is occupied during the simulation. Left : Gal/Rib linkage. Right : Rib/Kdn linkage. Similar results were observed for the other simulations, independently of the starting structure/force field.

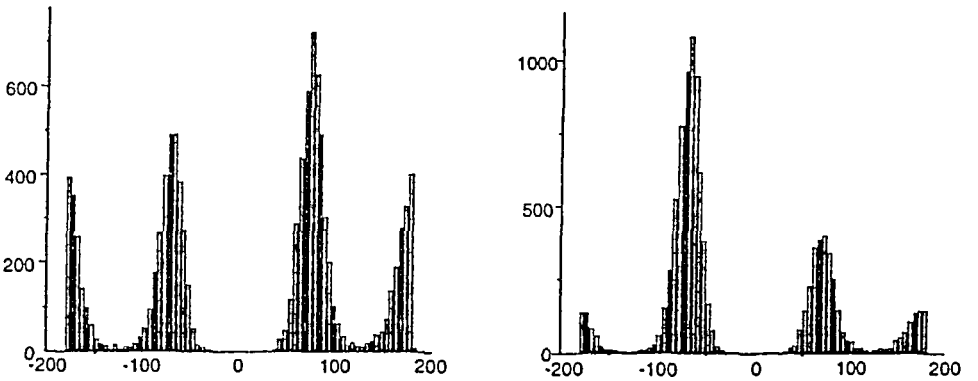

Figure 3. Histogram of the populations of *gg*, *gt*, and *tg* rotamers for Rib*f* (left) and Kdn*p* (right) hydroxymethyl chains during one 10 ns MD simulation with the MM3* force field (GB/SA). The starting structure has *gg* (Rib*f* and Kdn*p*) lateral chains.

those expected for the *exo*-anomeric effect,[21] although the expected probability distributions occupy a wide surface.[22]

Nine models of the trisaccharide **1** were then built, and submitted to different simulations using both force fields (see experimental). For all linkages, the glycosidic torsion angles cover a well defined part of the complete Φ/Ψ map (Fig. 2), which is fairly independent of the rotamer present for the hydroxymethyl groups. Independently of the force fields used, the glycosidic torsion angles Φ_{GR} and Ψ_{GR} show oscillations centered at -60 and -60 degrees. In all cases, these torsional oscillations are more pronounced around Ψ, as expected because the *exo*-anomeric effect restricts Φ. Minor excursions to the *anti* regions are evident. In addition, and also for both force fields, the glycosidic torsion angles Φ_{RK} and Ψ_{RK} show oscillations centered at 60° and 180°. Again, the torsional oscillations are more pronounced around Ψ. Most of the simulations showed stability around Ω angles. In order to evaluate more properly the accessible conformational space for the Ω linkages, two simulations of 10 ns each were also performed. The trajectories show now several transitions around the rotamers of the exocyclic chains (Fig. 3). A comparison between the observed NMR distribution and those predicted by MD is also presented in Table 3. It can be observed that the best match is observed when the MM3* force field is used for 10 ns. Finally, average expected interproton distances (Fig. 4) from the different MD simulations (Table 3)

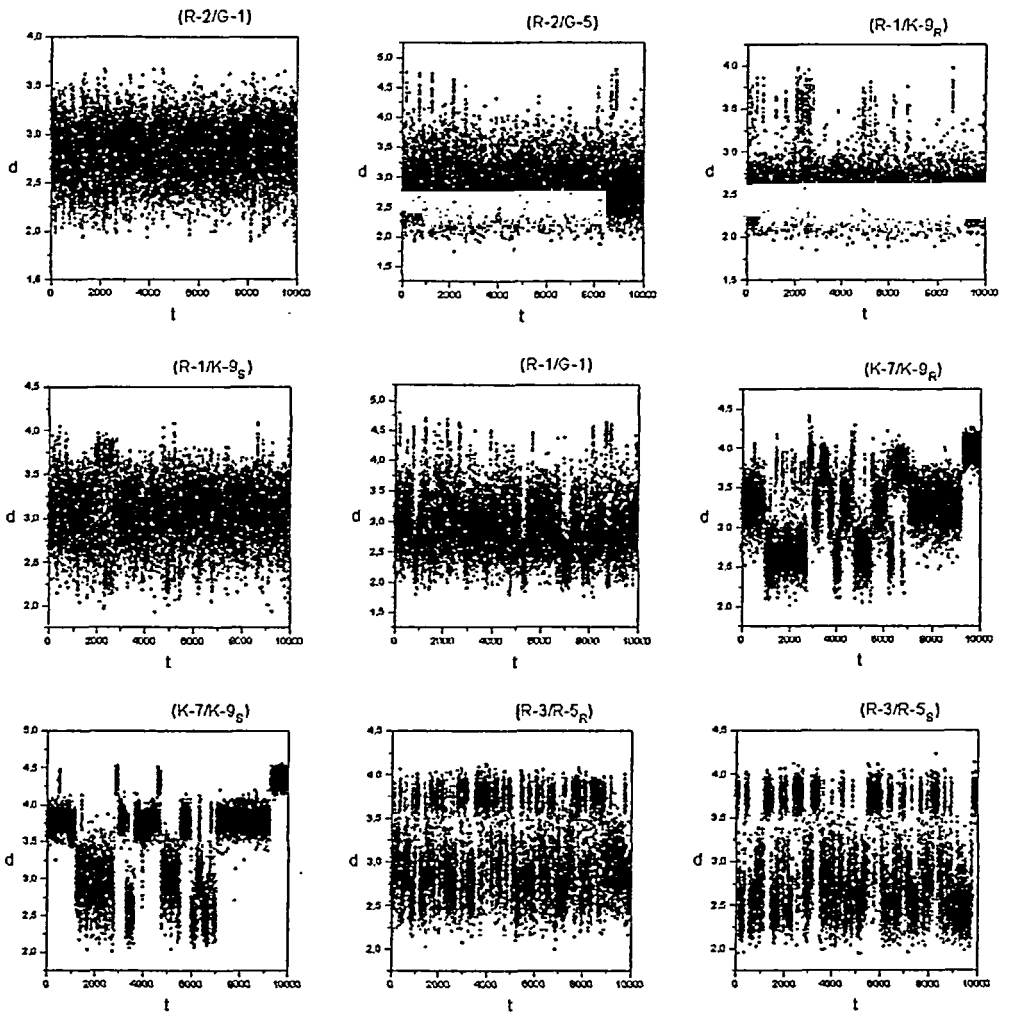

Figure 4. Trajectory plots of the key proton/proton distances which may be correlated with NOEs during a 10 ns MD simulation with the MM3* force field (GB/SA). The starting structure corresponds to *gg* (Rib*f*), *gt* (Gal*p*), and *gg* (Kdn*p*) lateral chains.

were estimated and compared to those observed experimentally. No close proton-proton distances were deduced from the MD models which were not apparent in the experimental NOE data. A superimposition of different conformers found in the MD simulation is shown in Figure 5. It is shown that despite the relatively narrow variation of the glycosidic torsion angles, the conformational space accessible to the trisaccharide

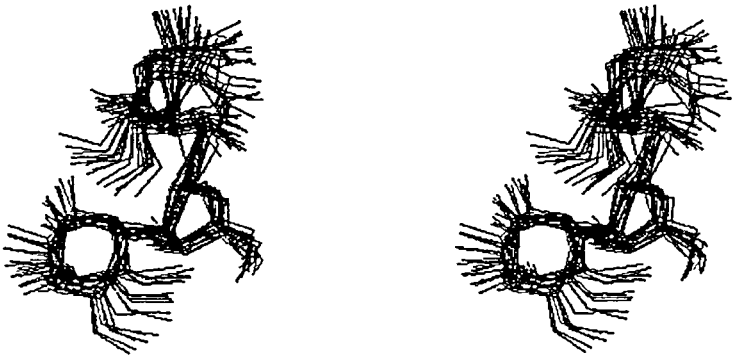

Figure 5. Superimposition of different conformers of **1**, found during one of the 10 ns MD simulation

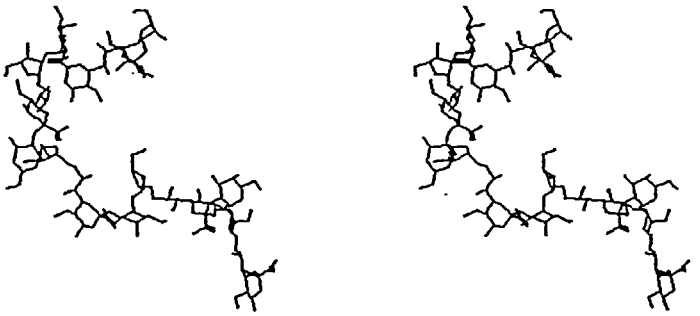

Figure 6. Stereoview of a possible conformation of the KPS polysaccharide

may be fairly large. A view of a putative conformation of the corresponding polysaccharide is shown in Figure 6.

CONCLUSION

Summarizing the experimental and computational results, it seems that there is an important amount of conformational freedom for the glycosidic and exocyclic torsion angles of the trisaccharides. Unrestrained MD simulations[23] provide a picture which agrees satisfactorily with the NMR experimental data. It can be deduced from this data that the nature of the receptor binding sites can easily modulate the conformational behaviour of this molecule.

ACKNOWLEDGMENT

Financial support by DGICYT (Grants PB96-0833 and BIO96-1469-C03) is gratefully acknowledged. We thank Dr. J. E. Ruiz-Sainz (Departamento de Microbiología, Facultad de Biología, Universidad de Sevilla) for supplying bacterial cultures. L. G. thanks Ministerio de Educacion y Ciencia for a postdoctoral fellowship.

REFERENCES

1. S. G. Wilkinson, *Prog. Lipid. Res.*, **35**, 283 (1996).
2. (a) B.L. Reuhs, R. W. Carlson, and J.S. Kim, *J. Biol. Chem.*, **175**, 3570 (1993); (b) J.S. Kim and B.L. Reuhs, *Abstracts of Papers*, Mol. Plant-Microbe Interact. 8th Int. MPMI Congress: 1996. Abstract 567.
3. A. M . Gil-Serrano, M. A. Rodríguez-Carvajal, P. Tejero-Mateo, J. L. Espartero, J. Thomas-Oathes, J. E. Ruiz-Sainz and A. M. Buendía-Claveria, *Biochem. J.*, **333** (1998), in press.
4. (a) T. J. Rutherford, D. G. Spackman, P. J. Simpson and S. W. Homans, *Glycobiology*, **4**, 59 (1994); (b) A. Poveda, J. L. Asensio, M. Martin-Pastor and J. Jimenez-Barbero, *J. Chem. Soc., Chem. Commun.*, 421 (1996).
5. A. Imberty, K. D. Hardman, J. P. Carver and S. Perez, *Glycobiology*, **1**, 456 (1991).
6. N.L Allinger, Y.H. Yuh and J.H. Lii, *J. Am. Chem. Soc.*, **111**, 8551 (1989).
7. F. Mohamadi, N. G. I. Richards, W. C. Guida, R. Liskamp, C. Canfield, G. Chang, T. Hendrickson and W. C. Still, *J. Comput. Chem.*, **11**, 440 (1990).
8. (a) K. Bock and J. Duus, *J. Carbohydr. Chem.*, **13**, 513 (1994); (b) G. D. Rockwell and T. B. Grindley, *J. Am. Chem. Soc.*, **120**, 10953 (1998).
9. W. C. Still, A. Tempczyk, R. C. Hawley and T. Hendrickson, *J. Am. Chem. Soc.*, **112**, 6127 (1990).
10. A. D. French and J. D. Brady, Eds., *Computer Modelling of Carbohydrate Molecules*, ACS Symp. Ser., 430; American Chemical Society: Washington, D.C., 1990.
11. J. Boyd, N. Soffe, B. John, D. Plant, and R. Hurd, *J. Magn. Reson.*, **98**, 660 (1992).
12. J. Ruiz-Cabello, G. W. Vuister, C. T. W. Moonen, P. van Gelderen, J. S. Cohen, and P. C. M. van Zihl, *J. Magn. Reson.*, **100**, 282 (1992).
13. A. Kumar, R. R. Ernst, and K. Wüthrich, *Biochem. Biophys. Res. Commun.*, **95**, 1 (1980).
14. A. A. Bothner-By, R. L. Stephens, J. M. Lee, C. D. Warren, and R. W. Jeanloz, *J. Am. Chem. Soc.*, **106**, 811 (1984).
15. T. L. Hwang and A. J. Shaka, *J. Am. Chem. Soc.*, **114**, 3157 (1992).
16. K. Stott, J. Stonehouse, J. Keeler, T.-L. Hwang, A. J. Shaka, *J. Am. Chem. Soc.*, **117**, 4199 (1995).
17. C. A. G. Haasnoot, F. A. A. M. de Leeuw and C. Altona, *Tetrahedron*, **36**, 2783 (1980).
18. D. Neuhaus and M. P. Williamson, *The Nuclear Overhauser Effect in Structural and Conformational Analysis*; VCH: New York (1989).

19. (a) S. W. Homans, *Biochemistry*, **29**, 9110 (1990); (b) C. Mukhopadhyay, K. E. Miller and C. A. Bush, *Biopolymers*, **34**, 21 (1994); (c) T. J. Rutherford, J. Partridge, C. T. Weller and S. W. Homans, *Biochemistry*, **32**, 12715 (1993); (d) H. C. Siebert, G. Reuter, R. Schauer, C. W. von der Lieth and J. Dabrowski, *Biochemistry*, **31**, 6962 (1992).
20. S. B. Engelsen, C. Herve du Penhoat and S. Perez, *J. Phys. Chem.*, **99**, 13334 (1995).
21. R. U. Lemieux, K. Bock, L. T. J. Delbaere, S. Koto and V .S. Rao, *Can. J. Chem.*, **58**, 631 (1980).
22. (a) B. R. Leeflang and L. M. J. Kroon-Batenburg, *J. Biomol. NMR*, **2**, 495 (1992); (b) J. P. M. Lommersee, L. M. J. Kroon-Batenburg, J. Kron, J. P. Kamerling and J. F. G. Vliegenthart, *J. Biomol. NMR*, **5**, 79 (1995).
23. (a) T. J. Rutherford and S. W. Homans, *Biochemistry*, **33**, 9606 (1994); (b) T. J. Rutherford, D. C. A. Neville and S. W. Homans, *Biochemistry*, **34**, 14131 (1995).